Received: 21 May 2016 | Revised: 27 September 2016 | Accepted: 7 November 2016

DOI 10.1002/poc.3675

WILEY Journal of Physical Organic Chemistry

RESEARCH ARTICLE

Synthesis, physicochemical, and biological activities of novel N-acyl tyrosine monomeric and Gemini surfactants in single and SDS/CTAB–mixed micellar system

Nausheen Joondan[1] | Sabina Jhaumeer-Laulloo[1] | Prakashanand Caumul[1] | Matthew Akerman[2]

[1] Department of Chemistry, Faculty of Science, University of Mauritius, Réduit, Mauritius

[2] University of KwaZulu-Natal, Pietermaritzburg, South Africa

Correspondence
Sabina Jhaumeer-Laulloo, Department of Chemistry, Faculty of Science, University of Mauritius, Réduit, Mauritius.
Email: sabina@uom.ac.mu

Abstract

A series of single-chained N-acyl tyrosine surfactants with varying chain lengths (C_{10}-C_{18}) and degree of unsaturation, as well as an N-acyl Gemini tyrosine surfactant with chain length C_{12}, were synthesized, and the structures were confirmed using spectral analysis. The effect of chain length and level of unsaturation on the physicochemical and antibacterial properties of the N-acyl tyrosine surfactants was evaluated. The C_{12} derivative displayed the optimum antibacterial activity among the single chain surfactants, and the presence of double bond in the oleoyl derivative enhanced the antibacterial activity over its saturated analogue. The N-acyl Gemini surfactant displayed the highest antibacterial activity among the series and also showed greater micelle forming ability than its single chain analogue. Mixed micellar behavior of the N-acyl Gemini surfactant with conventional cationic (CTAB) and anionic (SDS) surfactants in aqueous solution was studied. The negative value of the interaction parameter β_{12} observed for the N-acyl Gemini in binary mixture with CTAB surfactant indicated a synergistic interaction within the mixed micellar system. However, the binary mixture with SDS displayed antagonistic behavior. The binary mixture of N-acyl Gemini surfactant with CTAB displayed better antibacterial activity and foaming properties than with SDS mixtures. Optimum antibacterial activity was observed for N-acyl Gemini surfactant with mole ratio 0.4 to 0.6 in the CTAB binary mixture, at which the lowest ocular irritation index was observed. Overall, the study showed that the Gemini surfactant in combination with the conventional surfactant CTAB can be used as potential ingredients in detergent and pharmaceutical formulations.

KEYWORDS

critical micelle concentration, mixed micellar system, biological activity, N-acyl tyrosine surfactants

1 | INTRODUCTION

The strong demand towards the production of more environmentally benign chemicals has led to the use of greener alternatives to replace petroleum-based chemicals for the preparation of surfactants.[1] Amino acid–based surfactants have emerged as ecological, biocompatible, and renewable amphiphiles that have been applied in wide areas.[2–4]

Among the amino acid surfactants, the N-acyl amino acid derivatives are by far the most widely used in consumer product formulations because of their low toxicity and hypoallergenic, low irritancy, and high biodegradability.[5,6] In the N-acyl derivatives, the amide bonds are known to act as both hydrogen bond donors (the N–H moiety) and hydrogen bond acceptors (the C=O group) in intramolecular and intermolecular interactions during self-assembly in bulk and at surfaces to form various highly organized nanometer-scale structures.[7]

This class of surfactants has been thoroughly investigated with respect to dermatological properties and is generally regarded as safe with respect to skin irritation.[8] Moreover, N-acyl amino acid surfactants possess excellent physicochemical and antimicrobial activities, which render them valuable as additives in the formulation of food, detergents, cosmetics, personal care, and pharmaceutical products.[9,10]

The chemical and enzymatic syntheses of single chain and Gemini N-acyl surfactants derived from various amino acids have been reported in view of systematically producing surfactants with varying head groups. Sreenu et al[11] reported the synthesis, surface, and micellar properties of N-oleoyl surfactants derived from isoleucine and proline, and they were found to exhibit good surface tension reduction, emulsion stability, and calcium tolerance compared to conventional surfactants. N-decanoyl amino acid surfactants derived from leucine, methionine, serine, and proline were reported to exhibit favorable toxicity profiles.[12] N-acyl amino acids derived from the aromatic amino acid phenylalanine have also been reported, and these have been known to possess unique properties compared to other N-acyl amino acid surfactants.[13,14] From our previous studies, it was found that the O-alkyl esters of tyrosine showed enhanced physicochemical and antibacterial activities because of the presence of the phenolic group that enhances micellar formation and causes greater interaction with bacterial membrane.[15] However, to the best of our knowledge, there is no report on the systematic study of N-acyl derivatives derived from tyrosine.

This study reports the synthesis, physicochemical, and antibacterial activities of a series of N-acyl surfactants derived from tyrosine. The effect of chain lengths and presence of unsaturation of the fatty acid chain on the micellar and antibacterial properties were investigated. Mixed surfactant systems have been reported to have better properties than single surfactant systems. With this view, the physicochemical and biological activities of the N-acyl tyrosine surfactants in both single and mixed surfactant systems with conventional cetyl trimethyl ammonium bromide (CTAB) and sodium dodecyl sulfate (SDS) were evaluated. To be able to study their effectiveness as potential ingredients in detergents, the foaming properties as well as the ocular irritancy of the CTAB/SDS-N-acyl tyrosine surfactant mixtures were investigated.

2 | MATERIALS AND METHODS

2.1 | Chemicals and instrumentation

L-Tyrosine, decanoic acid, dodecanoic acid, tetradecanoic acid, palmitic acid, stearic acid, cetyl pyridinium chloride (CPC), and the fluorescence probe pyrene were purchased from Sigma-Aldrich (St. Louis, USA). Oleic acid and CTAB were obtained from BDH Laboratory Supplies (England). Silica gel (60-120 mesh) obtained from Alpha Chemika (India) was used for column chromatography. Mueller Hinton broth was obtained from Oxoid Ltd (United Kingdom). The different bacterial strains were obtained from Microbiologics (St. Cloud, Minnesota) and Oxoid Ltd (United Kingdom).

The ^{1}H NMR and ^{13}C NMR spectra were recorded at 250 and 62.9 MHz on a Bruker electro spin nuclear magnetic resonance spectrometer using $CDCl_3$, D_2O, and DMSO-d_6 as solvents. Infrared (IR) spectra were recorded on a Bruker Alpha Fourier transform infrared spectrometer. Fluorescence intensities were recorded on an LS 55 Perkin Elmer fluorescence spectrophotometer. Conductivity measurements were made using a Jenway 4320 conductivity meter. Elemental analysis was determined from a Eurovector EA3000 Elemental analyzer.

The X-ray data of compound **1** was recorded on a Bruker Apex Duo diffractometer equipped with an Oxford Instrument Cryojet operating at 100(2) K and an Incoatec microsource operating at 30-W power. The data were collected with Mo$K\alpha$ ($\lambda = 0.71073$ Å) radiation at a crystal-to-detector distance of 50 mm. The data collection was performed using omega and phi scans with exposures taken at 30-W X-ray power and 0.50° frame widths using APEX2.[16] The data were reduced with the program SAINT using outlier rejection, scan speed scaling, and standard Lorentz and polarization correction factors. A SADABS semiempirical multi-scan absorption correction was applied to the data. Direct methods, SHELX-2014[17] and WinGX,[18] were used to solve the data. All hydrogen atoms were included as idealized contributors in the least squares process. Their positions were calculated using a standard riding model with C–$H_{aromatic}$ distances of 0.93 Å and $U_{iso} = 1.2\ U_{eq}$, C–$H_{methylene}$ distances of 0.99 Å and $U_{iso} = 1.2\ U_{eq}$, and C–H_{methyl} distances of 0.98 Å and $U_{iso} = 1.5\ U_{eq}$. The O–H and N–H atoms were located in the difference density map and refined isotropically. Crystal and structure refinement data of compound **1** are given in Table 1.

2.2 | Synthesis and characterization

N-acyl tyrosine surfactants were synthesized by the reaction of the tyrosine ester with selected fatty acid (butanoic, decanoic, dodecanoic, tetradecanoic, palmitic, stearic, and oleic acids) chlorides of varying chain lengths. The corresponding fatty acid chloride (1.5 eq) was added to a solution of L-Tyrosine ester (4.31 mmol) and triethylamine (3.2 mL) in tetrahydrofuran (70 mL) followed by a catalytic amount of 4-dimethylaminopyridine. The mixture was refluxed for 18 hours and then quenched with water (100 mL). The organic phase was extracted with ethyl acetate. The combined organic extracts were washed with sodium bicarbonate (5%, 50 mL) and dried over anhydrous magnesium sulfate, and the solvent was removed in vacuo. The crude product was washed with excess ether to give the corresponding N-acyl derivative as white solid.

TABLE 1 Crystal and structure refinement data of compound **1**

Crystal Data	Compound 1
Chemical formula	$C_{14}H_{19}NO_4$
Molar mass (g mol^{-1})	265.30
Crystal system, space group	Orthorhombic, $P2_12_12_1$
Temperature (K)	100(2)
a, b, c (Å)	8.6205(8), 14.9938(12), 22.1253(18)
α, β, γ (°)	$\alpha = \beta = \gamma = 90$
V (Å^3)	2859.8(4)
Z	8
Radiation type	Mo$K\alpha$
μ (mm^{-1})	0.09
Crystal size (mm)	0.39 × 0.28 × 0.11
Data Collection	
Diffractometer	Bruker Apex Duo CCD diffractometer
Absorption correction	Multi-scan, SADABS, Bruker 2012
T_{min}, T_{max}	0.679, 0.745
No. of measured, independent, and observed [$I > 2\sigma(I)$] reflections	18931, 5710, 5483
R_{int}	0.021
Refinement	
$R[F^2 > 2\sigma(F^2)]$, $wR(F^2)$, S	0.029, 0.072, 1.06
No. of reflections	5710
No. of parameters	364
No. of restraints	0
H-atom treatment	H atoms treated by a mixture of independent and constrained refinement
$\Delta\rho_{max}$, $\Delta\rho_{min}$ (e Å^{-3})	0.17, −0.15
Absolute structure	Refined as an inversion twin
Absolute structure parameter	0.2(8)

2.2.1 | N-butyroyl L-tyrosine methyl ester 1

Yield: 63%.^{1}H NMR ($CDCl_3$), δ (ppm): 0.87 (t, J 7 Hz, 3H, $COCH_2CH_2C\underline{H}_3$), 1.59 (m, 2H, $COCH_2C\underline{H}_2CH_3$), 2.15 (m, 2H, $COC\underline{H}_2CH_2CH_3$), 3.00 (2H, m, CH_2Ph), 3.70 (s, 3H, OCH_3), 4.85 (m, 1H, CH), 5.98 (d, J 8 Hz, 1H, N–H), 6.73 (d, J 8 Hz, 2H, Ph), 6.92 (d, J 8 Hz, 2H, Ph). ^{13}C NMR ($CDCl_3$), δ (ppm): 13.7 ($COCH_2CH_2\underline{C}H_3$), 19.0 ($COCH_2C\underline{H}_2CH_3$), 37.2 ($COCH_2C\underline{H}_2CH_3$), 38.4 ($CH_2Ph$), 52.4 ($O\underline{C}H_3$), 53.1 (CH), 115.6, 127.0, 130.3, 155.6 (C_6H_4), 172.4, 173.1(C=O).

2.2.2 | N-decanoyl L-tyrosine methyl ester 2

Yield: 68%. Elem Anal Found: C, 67.14; H, 8.98; N, 3.70; Calcd for $C_{20}H_{31}NO_4$: C, 67.74; H, 8.94; N, 4.01. GC-MS, m/z: 349.93. IR, ν_{max} (cm^{-1}): 3333, 1749, 1646. ^{1}H NMR ($CDCl_3$), δ (ppm): 0.89 (t, J 7 Hz, 3H, $CO(CH_2)_8C\underline{H}_3$), 1.27 (m, 12H, $COCH_2CH_2(C\underline{H}_2)_6CH_3$), 1.62 (m, 2H, $COCH_2C\underline{H}_2(CH_2)_6CH_3$), 2.19 (m, 2H, $COC\underline{H}_2(CH_2)_7CH_3$), 3.03 (dd, J 14 Hz, J 7 Hz, 1H, C$\underline{H}$HPh), 3.05 (dd, J 14 Hz, J 7 Hz, 1H, CH$\underline{H}$Ph), 3.74 (s, 3H, OCH_3), 4.89 (m, 1H, C$\underline{H}$), 5.97 (d, J 8 Hz, 1H, N–H), 6.76 (d, J 8 Hz, 2H, Ph), 6.96 (d, J 8 Hz, 2H, Ph). ^{13}C NMR ($CDCl_3$), δ (ppm): 14.1 ($CO(CH_2)_8\underline{C}H_3$), 22.7 to 31.9 ($COCH_2(\underline{C}H_2)_7CH_3$), 36.6 ($CO\underline{C}H_2(CH_2)_7CH_3$), 37.3 ($CH_2Ph$), 52.4 ($O\underline{C}H_3$), 53.1 (CH), 115.5, 127.2, 130.3, 155.4 (C_6H_4), 172.4, 173.3 (C=O).

2.2.3 | N-dodecanoyl L-tyrosine methyl ester 3

Yield: 73%. Elem Anal Found: C, 69.22; H, 10.46; N, 3.94; Calcd for $C_{22}H_{35}NO_4$: C, 69.49; H, 9.84; N, 3.71. GC-MS, m/z: 377.14. IR, ν_{max} (cm^{-1}): 3334, 1749, 1646. ^{1}H NMR ($CDCl_3$), δ (ppm): 0.89 (t, J 7 Hz, 3H, $CO(CH_2)_{10}C\underline{H}_3$), 1.27 (m, 16H, $COCH_2CH_2(C\underline{H}_2)_8CH_3$), 1.60 (m, 2H, $COCH_2C\underline{H}_2(CH_2)_8CH_3$), 2.19 (m, 2H, $COC\underline{H}_2(CH_2)_9CH_3$), 3.06 (dd, J 14 Hz, J 7 Hz, 1H, C$\underline{H}$HPh), 3.12 (dd, J 14 Hz, J 7 Hz, 1H, CH$\underline{H}$Ph), 3.75 (s, 3H, OCH_3), 4.88 (m, 1H, C$\underline{H}$), 5.92 (d,J 8 Hz, 1H, NH), 6.77 (d, J 8 Hz, 2H, Ph), 6.98 (d, J 8 Hz, 2H, Ph). ^{13}C NMR ($CDCl_3$), δ (ppm): 14.1 ($CO(CH_2)_{10}\underline{C}H_3$), 22.7 to 31.9 ($COCH_2(\underline{C}H_2)_9CH_3$), 36.6 ($CO\underline{C}H_2(CH_2)_9CH_3$), 37.3 ($CH_2Ph$), 52.4 ($O\underline{C}H_3$), 53.1 (CH), 115.5, 127.3, 130.3, 155.3 (C_6H_4), 172.4, 173.2 (C=O).

2.2.4 | N-tetradecanoyl L-tyrosine methyl ester 4

Yield: 54%. Elem Anal Found: C, 72.40; H, 11.87; N, 2.88; Calcd for $C_{24}H_{39}NO_4$: C, 71.97; H, 11.69; N, 2.45. IR, ν_{max} (cm^{-1}): 3376, 2949, 1736. ^{1}H NMR ($CDCl_3$), δ (ppm): 0.89 (t, J 7 Hz, 3H, $CO(CH_2)_{12}C\underline{H}_3$), 1.27 (m, 20H, $COCH_2CH_2(C\underline{H}_2)_{10}CH_3$), 1.63 (m, 2H,

$COCH_2\underline{CH_2}(CH_2)_{10}CH_3$), 2.22 (m, 2H, $COCH_2\underline{(CH_2)_{11}CH_3}$), 3.07 (m, 2H, CH_2Ph), 3.74 (s, 3H, OCH_3), 4.89 (m, 1H, $C\underline{H}$), 5.93 (d, *J* 8 Hz, 1H, NH), 6.77 (d, *J* 8 Hz, 2H, Ph), 6.99 (d, *J* 8 Hz, 2H, Ph). ^{13}C NMR ($CDCl_3$), δ (ppm): 14.1 ($CO(CH_2)_{12}\underline{CH_3}$), 22.7 to 31.9 ($COCH_2\underline{(CH_2)_{11}CH_3}$), 36.6 ($CO\underline{CH_2}(CH_2)_7CH_3$), 37.3 ($CH_2Ph$), 52.4 ($O\underline{CH_3}$), 52.9 ($C\underline{H}$), 115.6, 127.5, 130.3, 155.3 (C_6H_4), 172.4, 173.0 (C=O).

2.2.5 | N-palmitoyl L-tyrosine methyl ester 5

Yield: 71%. Elem Anal Found: C, 72.16; H, 10.87; N, 4.20; Calcd for $C_{26}H_{43}NO_4$: C, 72.02; H, 10.00; N, 3.93. IR, ν_{max} (cm^{-1}): 3376, 2949, 1736. ^{1}H NMR ($CDCl_3$), δ (ppm): 0.89 (t, *J* 7 Hz, 3H, $CO(CH_2)_{14}\underline{CH_3}$), 1.26 (m, 24H, $COCH_2CH_2\underline{(CH_2)_{12}CH_3}$), 1.57 (m, 2H, $COCH_2\underline{CH_2}(CH_2)_{12}CH_3$), 2.19 (m, 2H, $CO\underline{CH_2}(CH_2)_{13}CH_3$), 3.04 (m, 2H, CH_2Ph), 3.75 (s, 3H, OCH_3), 4.87 (m, 1H, $C\underline{H}$), 5.90 (d, *J* 8 Hz, 1H, NH), 6.73 (d, *J* 8 Hz, 2H, Ph), 6.97 (d, *J* 8 Hz, 2H, Ph). ^{13}C NMR ($CDCl_3$), δ (ppm): 14.1 ($CO(CH_2)_{12}\underline{CH_3}$), 22.7 to 31.9 ($COCH_2\underline{(CH_2)_{11}CH_3}$), 36.6 ($CO\underline{CH_2}(CH_2)_7CH_3$), 37.2 ($CH_2Ph$), 52.4 ($O\underline{CH_3}$), 53.1 ($C\underline{H}$), 115.5, 127.6, 130.4, 155.0 (C_6H_4), 172.4, 172.9 (C=O).

2.2.6 | N-stearoyl L-tyrosine methyl ester 6

Yield: 65%. Elem Anal Found: C, 71.95; H, 11.91; N, 3.20; Calcd for $C_{28}H_{47}NO_4$: C, 72.34; H, 11.26; N, 3.03. IR, ν_{max} (cm^{-1}): 3376, 2949, 1736 ^{1}H NMR ($CDCl_3$), δ (ppm): 0.89 (m, 3H, $CO(CH_2)_{16}\underline{CH_3}$), 1.26 (m, 28H, $COCH_2CH_2\underline{(CH_2)_{14}CH_3}$), 1.61 (m, 2H, $COCH_2\underline{CH_2}(CH_2)_{14}CH_3$), 2.19 (m, 2H, $CO\underline{CH_2}(CH_2)_{15}CH_3$), 3.05 (m, 2H, CH_2Ph), 3.74 (s, 3H, OCH_3), 4.87 (m, 1H, $C\underline{H}$), 5.97 (d, *J* 8 Hz,1H, NH), 6.74 (d, *J* 8 Hz, 2H, Ph), 6.95 (d, *J* 8 Hz, 2H, Ph). ^{13}C NMR ($CDCl_3$), δ (ppm): 14.1 ($CO(CH_2)_{16}\underline{CH_3}$), 22.7 to 31.9 ($COCH_2\underline{(CH_2)_{15}CH_3}$), 36.6 ($CO\underline{CH_2}(CH_2)_{15}CH_3$), 37.2 ($CH_2Ph$), 52.4 ($O\underline{CH_3}$), 53.1 ($C\underline{H}$), 115.5, 127.5, 130.4, 155.1 (C_6H_4), 172.4, 173.0 (C=O).

2.2.7 | N-oleoyl L-tyrosine methyl ester 7

Yield: 78%. IR, ν_{max} (cm^{-1}): 3376, 2949, 1736. ^{1}H NMR ($CDCl_3$), δ (ppm): 0.86 (m, 3H, $CO(CH_2)_7$–CH=CH–$(CH_2)_7\underline{CH_3}$), 1.25 (m, 20H, $COCH_2CH_2\underline{(CH_2)_4}CH_2$–CH=CH–$CH_2\underline{(CH_2)_6}CH_3$), 1.54 (m, 2H, $COCH_2\underline{CH_2}(CH_2)_4CH_2$–CH=CH–$CH_2(CH_2)_6CH_3$), 2.16 (m, 2H, $CO\underline{CH_2}(CH_2)_6$–CH=CH–$(CH_2)_7\underline{CH_3}$), 3.00 (m, 2H, CH_2Ph), 3.71 (s, 3H, OCH_3), 4.86 (m, 1H, $C\underline{H}$), 5.34 (m, 2H, $CO(CH_2)_7$–$C\underline{H}$=$C\underline{H}$–$(CH_2)_7CH_3$), 5.96 (d, *J* 8 Hz, 1H, NH), 6.73 (d, *J* 8 Hz, 2H, Ph), 6.93 (d, *J* 8 Hz, 2H, Ph). ^{13}C NMR ($CDCl_3$), δ (ppm): 14.1 ($CO(CH_2)_7$–CH=CH–$(CH_2)_7\underline{CH_3}$), 22.7 to 31.9 ($COCH_2\underline{(CH_2)_6}$–CH=CH–$\underline{(CH_2)_7CH_3}$), 36.6 ($CO\underline{CH_2}(CH_2)_6$–CH=CH–$(CH_2)_7CH_3$), 37.3 ($CH_2Ph$), 52.4 ($O\underline{CH_3}$), 53.2 ($C\underline{H}$), 115.6, 127.0, 130.3, 155.6 (C_6H_4), 129.8, 130.0 ($CO(CH_2)_7$–$C\underline{H}$=$C\underline{H}$–$(CH_2)_7CH_3$), 172.4, 173.3 (C=O).

2.2.8 | N-dodecanoyl L-tyrosine dodecyl ester 8

Yield: 77%. Elem Anal Found: C, 73.425; H, 10.60; N, 4.82; Calcd for $C_{33}H_{57}NO_4$: C, 73.53; H, 10.80; N, 4.63. ESI-MS, m/z: 554.42 (M+ Na^+). IR, ν_{max} (cm^{-1}): 3376, 2949, 1736. ^{1}H NMR (DMSO), δ (ppm): 0.85 (m, 3H, $CO(CH_2)_{10}\underline{CH_3}$), 0.85 (m, 3H, $O(CH_2)_{11}\underline{CH_3}$), 1.23 (m, 16H, $COCH_2CH_2\underline{(CH_2)_8}CH_3$), 1.23 (m, 18H, $OCH_2CH_2\underline{(CH_2)_9}CH_3$), 1.47 (m, 2H, $COCH_2\underline{CH_2}(CH_2)_8CH_3$), 1.47 (m, 2H, $OCH_2\underline{CH_2}(CH_2)_9CH_3$), 2.03 (m, 2H, $COCH_2\underline{(CH_2)_9}CH_3$), 2.78 (m, 2H, CH_2Ph), 3.96 (t, *J* 7 Hz, 3H, $OCH_2\underline{(CH_2)_{10}}CH_3$), 4.32 (m, 1H, $C\underline{H}$), 6.63 (d, *J* 8 Hz, 2H, Ph), 6.98 (d, *J* 8 Hz, 2H, Ph), 8.15 (d, *J* 8 Hz, 1H, NH), 9.25 (s, 1H, OH). ^{13}C NMR ($CDCl_3$), δ (ppm): 14.1 ($CO(CH_2)_{10}\underline{CH_3}$), 14.1 ($O(CH_2)_{11}\underline{CH_3}$), 22.7 to 31.9 ($COCH_2\underline{(CH_2)_9}CH_3$), 22.7 to 31.9 ($OCH_2\underline{(CH_2)_{10}}CH_3$), 35.5 ($CH_2Ph$), 36.5 ($CO\underline{CH_2}(CH_2)_9CH_3$), 54.5 ($C\underline{H}$), 64.8 ($O\underline{CH_2}(CH_2)_{10}CH_3$), 115.5, 127.8, 130.4, 156.5 (C_6H_4), 172.4, 173.7 (C=O).

2.3 | Critical micelle concentration determination

2.3.1 | Critical micelle concentration determination of 2-8

Pyrene was used as a fluorescence probe to determine the critical micelle concentration (CMC) of the N-acyl tyrosine surfactants (compounds **2**-**8**) in aqueous solution at 25°C. Stock solution of pyrene in methanol (10 μL, 0.1mM) was transferred into vials. After evaporating the methanol, surfactant solutions (3 mL) of varying concentrations were added to the vials to give a final concentration of 1.6μM of pyrene in each vial. Fluorescence spectra of pyrene were recorded over the spectral range 350 to 450 nm. The excitation wavelength was kept at 334 nm, and the emission was recorded at 373 (I_1) and 384 (I_3) nm. The ratio of the intensities of the first and third vibronic peaks in the fluorescence spectrum of pyrene (I_1/I_3) was recorded as a function of the N-acyl surfactant concentrations to determine the CMCs.

2.3.2 | Critical micelle concentration determination of SDS/CTAB–8 mixed system.

Mixed SDS-**8** systems with varying mole fractions of **8** (0, 0.2, 0.4, 0.6, 0.8, 1) were prepared by mixing precalculated volumes of the stock solutions of SDS and **8** in water, and the solutions were stirred for 1 hour. Mixed CTAB-**8** systems were also prepared in a similar way, and the mole fraction of **8** in the mixed solution was expressed as

$$\alpha_8 = \frac{[8]}{[8] + [\mathrm{SDS/CTAB}]}$$

where [**8**], [SDS], and [CTAB] are the concentrations of the Gemini surfactant **8**, SDS, and CTAB in the mixed solutions, respectively.

The CMC of the different mixed systems was determined via conductivity measurements by adding successive

amounts of the stock solutions to deionized water in the form of a titration.

2.4 | Aggregation number

Pyrene solution in methanol (10 μL, 0.1mM) was pipetted into 4-mL vials. After evaporating the methanol, 10 μL of aqueous quencher solution, CPC of varying concentration (0M-0.3M) was pipetted into the pyrene followed by the surfactant (**2-8**) solution (3 mL), with concentration 5 times above their respective CMC values. The fluorescence intensities of pyrene in the different solutions were then measured at 373 nm.

2.5 | Krafft temperature

To measure the Krafft temperature of the CTAB**-8** system, 0.01-M solutions of varying mole fractions of surfactant **8** (0, 0.2, 0.4, 0.6, 0.8) were prepared in deionized water and placed in the refrigerator for 24 hours at 4°C. The conductivity was noted as the temperature of the solution was raised under gentle stirring.

2.6 | Antibacterial activity

The antibacterial activities were determined against 3 gram-positive strains, namely, *Staphylococcus aureus* (ATCC 25923), *Staphylococcus epidermidis* (ATCC 12228), and *Bacillus cereus* (ATCC 11778, ATCC 10876), and 3 gram-negative strains, namely, *Klebsiella pneumoniae* (ATCC 13883), *Escherichia coli* (ATCC 22922), and *Salmonella typhimurium* (ATCC 14028), using the broth dilution method.[19] The antibacterial activity was expressed as the minimum inhibitory concentration (MIC) that was defined as the lowest concentration that inhibits the growth of bacteria. Cetyl trimethyl ammonium bromide and sodium dodecyl sulfate were used as positive controls. The antibacterial activities of the different SDS/CTAB**–8** mixed micelle systems ($\alpha_{\mathbf{8}} = 0$, 0.2, 0.4, 0.6, and 0.8) were determined starting from solutions with a total surfactant concentration (C_T) of 0.05M ([**8**] + [SDS] or [CTAB]).

All wells were inoculated with 50 μL of a bacterial suspension adjusted to 0.5 McFarland in physiological solution. Microplates were covered and incubated for 24 hours at 37°C. The MIC of the surfactants was detected following addition of 20-μL iodonitrotetrazolium chloride (0.4 mg mL^{-1}) and incubation at 37°C for 30 minutes. Viable microorganisms reduced the yellow dye to a pink color. Minimum inhibitory concentration was defined as the lowest sample concentration that prevented this change and exhibited complete inhibition of bacterial growth.

2.7 | Foamability measurements

The surfactant solutions (20 mL, 0.1 wt%) were shaken vigorously for 10 seconds in a calibrated 100-mL glass cylinder with a stopper, and the height of the foam formed was measured. The different SDS/CTAB**–8** ($\alpha_{\mathbf{8}} = 0$, 0.2, 0.4, 0.6, 0.8, and 1) mixed systems (5 mL, 500mM) were shaken vigorously for 10 seconds in a calibrated 10-mL glass cylinder, and the height of the foam was recorded. All the measurements were performed at 25°C in triplicate, and the results were reported as the mean value ± standard deviation.

3 | RESULTS AND DISCUSSION

3.1 | Synthesis and characterization

A series of N-acyl surfactants derived from L-Tyrosine were synthesized by the condensation of tyrosine ester with fatty acid chlorides of varying chain lengths (C_4 and C_8-C_{18}) (Figure 1).

In previous reports, the N-acyl amino acid surfactants were synthesized by the Schotten-Baumann reaction, whereby NaOH in tetrahydrofuran/water was used.[20] In this study, a milder base (triethylamine) was used for the synthesis of the N-acyl tyrosine surfactants because of the presence of the ester moiety that is sensitive to hydrolysis. All the N-acyl tyrosine surfactants were solids at room temperature, and the chemical structures were confirmed by ^{1}H NMR, ^{13}C NMR, IR spectra, GC-MS, MS, and elemental analysis.

The presence of the new carbonyl signal at δ 172.7 to 173.7 ppm in the ^{13}C NMR and at 1645 to 1647 cm^{-1} in the IR spectra confirmed the formation of the N-acyl surfactants.

To study the effect of the presence of an unsaturated system in the hydrophobic tail of the N-acyl surfactants, tyrosine methyl ester was made to react with oleoyl chloride, leading to the formation of N-oleoyl tyrosine methyl ester **7**. The presence of the unsaturated system was confirmed by a multiplet at δ 5.34 ppm in the ^{1}H NMR spectrum corresponding to the 2 olefinic protons.

In view of producing Gemini-like amphiphiles, N-acylation was performed on a longer chain tyrosine ester, to produce an amphiphile with a double tail system having chain length C_{12} at both the N-acyl and O-ester moieties (**8**).

The surfactant **8** (Figure 2) was found to possess the molecular formula $C_{33}H_{57}NO_4$. The ^{13}C NMR spectrum showed 18 signals, 4 from which correspond to the aromatic segment. The 2 signals in the ^{13}C NMR with the highest chemical shift, 172.4 and 172.7 ppm, correspond to the carbonyl groups C**-13** and C-**16**, respectively. In the aromatic segment, magnetically equivalent carbon atoms C-**30** and C-**34** appear at δ 130.4 ppm, while C-**31** and C-**33** appear at δ 115.4 ppm in the ^{13}C NMR spectrum. These assignments were confirmed by bidimentional techniques (Homonuclear correlation spectroscopy (COSY), Heteronuclear single-quantum correlation spectroscopy (HSQC) and Heteronuclear multiple-bond correlation spectroscopy (HMBC)).The selected data are shown in Table 2.

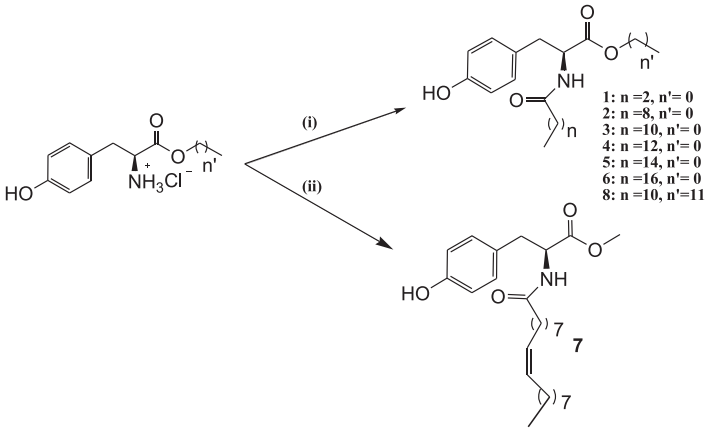

FIGURE 1 Synthesis of N-acyl tyrosine surfactants **1-8**

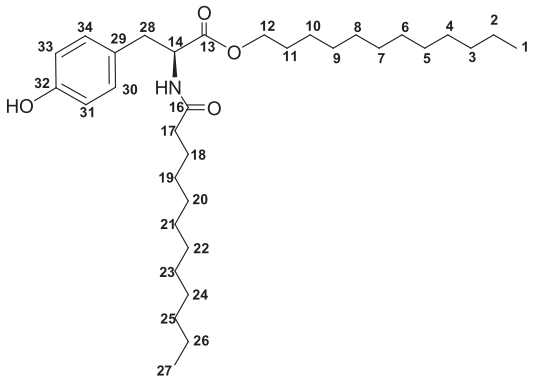

FIGURE 2 Labelled structure of Gemini surfactant **8**

3.1.1 | X-ray structure of compound 1

Compound **1** crystallized in the orthorhombic space group $P2_12_12_1$ with 2 molecules linked through a hydrogen bond in the asymmetric unit (ie, $Z = 8$) as shown in Figure 3.

The key structural difference between the 2 molecules in the asymmetric unit is the relationship between the amide N atom and ester groups. In one molecule (as shown in Figure 3), the carbonyl oxygen atom is *trans* to the amide N atom and in the second molecule the geometry is *cis*. By inspection, it would appear that neither geometry leads to significant steric strain within the molecule and therefore, the energy difference between the 2 geometries is likely to be modest.

The mean C=O bond length of the amide group measures 1.214(3), this coupled with the N–C–O and C–C–O bond lengths which average 121.0(3)° and 122.5(3)° illustrate the sp^2 hybridized nature of the amide carbon atom.

The molecule exhibits a number of intermolecular hydrogen bonds. Firstly, the 2 molecules A and B in the asymmetric unit are linked through a hydrogen bond between the hydroxy groups of the 2 adjacent molecules. One hydroxy group acts as the H-bond donor and the other as the H-bond

TABLE 2 Selected spectral data of compound **8**

Atom	δ (^{1}H) ppm	^{1}H–^{1}H COSY	δ (^{13}C) ppm	DEPT (Distortionless enhancement by polarization transfer)	HMBC
12	3.96 (t, 7 Hz, 2H)	11	64.8	CH_2	13[b]
13			172.4		
14	4.32 (m, 1H)	15, 28	54.5	CH	13[a]
15	8.17 (d, 7.7 Hz, N–H)	14			16[a]
16			172.7		15[a], 17[a]
17	2.02 (t, 7.5 Hz, 2H)	18	35.5	CH_2	16[a]
28	2.78 (dd, *J* 14 Hz, *J* 7 Hz, 1H, CH_2Ph)	14	36.5	CH_2	29[a], 30[b], 34[b]
29			127.8	C	
30	6.98 (d, *J* 8 Hz, 1H, Ph)	31	130.4	CH	29[a], 31[a], 33[a], 32[b]
31	6.63 (d, *J* 8 Hz, 1H, Ph),	30	115.4	CH	30[a], 32[b], 33[b]
32			156.5	C	
33	6.63 (d, *J* 8 Hz, 1H, Ph),	34	115.4	CH	31[b], 32[a], 34[a]
34	6.98 (d, *J* 8 Hz, 1H, Ph)	33	130.4	CH	29[a], 33[a], 30[b], 32[b]

[a]2-bond correlation.

[b]3-bond correlation.

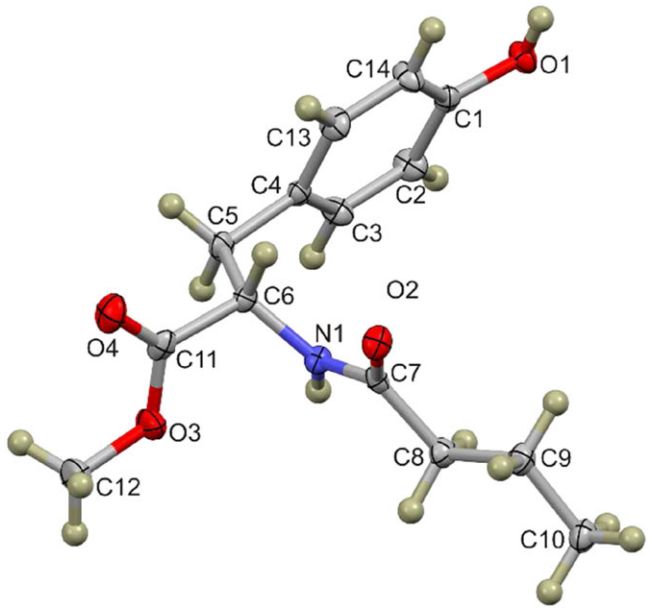

FIGURE 3 Displacement ellipsoid plot (50% probability) of compound **1**. For clarity, a single molecule from the asymmetric unit has been shown. Hydrogen atoms are drawn as spheres of arbitrary radius

acceptor. In addition to this hydrogen bond, there are 3 additional hydrogen bonds. One of the amide NH groups is hydrogen-bonded to the amide carbonyl oxygen of an adjacent molecule and the other to one of the hydroxy groups. The final hydrogen bond is between one of the hydroxy groups and the amide carbonyl of an adjacent molecule. Each of the hydroxy groups therefore acts as both an H-bond acceptor and an H-bond donor; the oxygen atoms of the ester groups are not involved in H-bonds. These interactions link 5 molecules, as shown in Figure 4. The hydrogen bond parameters are summarized in Table 3.

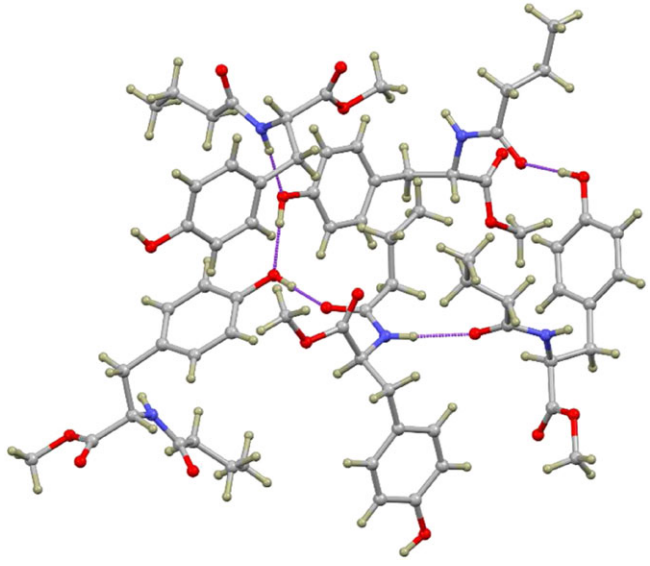

FIGURE 4 Hydrogen bonding of compound **1**. The 4 hydrogen bonds stabilize a 3-dimensional supramolecular structure. Hydrogen bonds are shown as dashed purple tubes

TABLE 3 Hydrogen bond parameters for compound **1**

Bond	D–H (Å)	H···A (Å)	D···A (Å)	D–H···A (°)
O5–H103···O1	0.87(3)	1.78(3)	2.649(2)	173(3)
O1–H104···O6	0.80(4)	2.60(4)	3.384(3)	179(3)
N1–H101···O5	0.87(2)	2.06(3)	2.922(2)	171(2)
N2–H102···O2	0.89(2)	1.98(2)	2.859(2)	169(5)

The hydrogen bond distances summarized in Table 2 are significantly shorter than the sum of the van der Waals radii. The D···A bond lengths are shorter than the sum of the van der Waals radii by 0.661 to 1.010 Å; this is a significant difference when compared to previously reported hydrogen bonds[21] and suggests that the interaction is likely strong. This is further supported by the fact that the hydrogen bond angles do not deviate significantly from the ideal angle of 180°. The 4 hydrogen bonds stabilize a 3-dimensional supramolecular structure that packs in alternating layers of molecules A and B as shown in Figure 5.

3.2 | Critical micelle concentration and aggregation number of 2-8

The critical micelle concentration of the synthesized N-acyl tyrosine surfactants **2-8** was determined by fluorescence study using pyrene as probe. Pyrene molecules are highly hydrophobic, and in micellar solution, they are preferentially solubilized within the hydrophobic interior of the aggregates and are strongly distributed into the micelle as soon as they form.[22]This causes an abrupt decrease in the I_1/I_3 ratio at the onset of micellar formation when a surfactant is added to an aqueous solution of pyrene. Figure 6 represents the fluorescence spectrum of pyrene in the presence of the N-acyl tyrosine surfactant **3**.

The micellar aggregation number (*N*ss) of the N-acyl tyrosine surfactants **2-8** was determined by steady-state fluorescence quenching technique, using pyrene as probe and

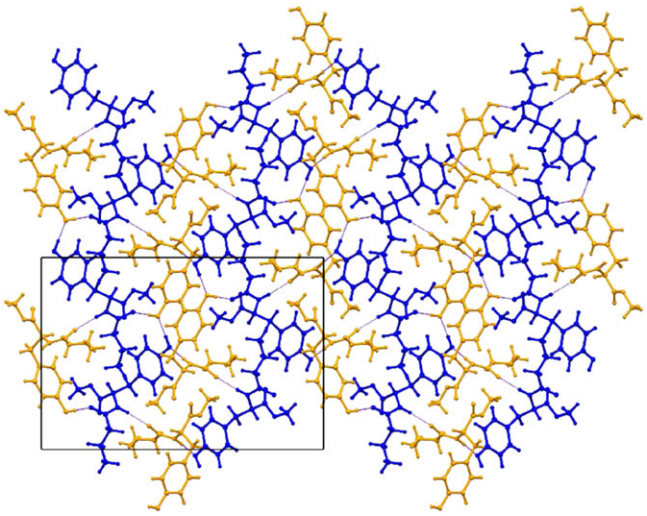

FIGURE 5 Alternating layers of molecules A and B in the 3-dimensional supramolecular structure supported by extensive hydrogen bonding

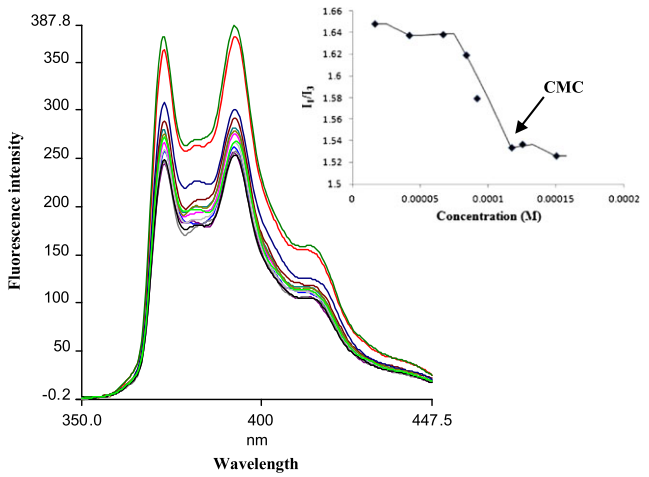

FIGURE 6 CMC determination of N-decanoyl tyrosine methyl ester (**3**). CMC indicates ritical micelle concentration

CPC as quencher. The aggregation numbers were determined by using Equations 1 and 2.

$$N_{SS} = \left(\frac{C-\text{CMC}}{[\text{Micelle}]}\right) \quad (1)$$

$$\frac{I_0}{I_Q} = \exp\left(\frac{[Q]}{[\text{Micelle}]}\right) \quad (2)$$

where I_0 and I_Q are the fluorescence intensities in the absence and presence of CPC, respectively, C is the concentration of surfactant added, and $[Q]$ is the concentration of the quencher CPC. The concentration of micelles [Micelle] was calculated from the plot of ln (I_0/I_Q) versus $[Q]$ and replaced in Equation 1 to determine *N*ss.

The CMC and the aggregation numbers (*N*ss) of the N-acyl surfactants are shown in Table 4.

As expected, increasing the chain length of the N-acyl tyrosine surfactants causes a decrease in the CMC and an increase in aggregation number because of the greater hydrophobicity of the molecules. The presence of an unsaturated system in the alkyl chain of **7** was found to increase the CMC of the surfactant as previously reported, compared to its analogous saturated derivative **6**.[23] This is due to the increase in the bulkiness and rigidity of the chain causing a loss in the degree of rotational freedom, which interferes with the tight packing of the tails in the micelle.[24] The increase in CMC may also be due to the decrease in hydrophobicity of the chain because of the delocalized π electrons that causes an increase in the polarizability of the chain and hence decreases the ease of micellization.

The presence of a second hydrophobic chain in the Gemini surfactant **8** causes a decrease in the CMC of the surfactant compared to its single chain analogue **3**, because of an increase in hydrophobic character of the surfactant that enhances micellar formation.

Mixed surfactant systems are known to influence physical properties of the individual components, and these systems are encountered in several applications.[25,26] Mixed surfactant systems in water undergo several physicochemical changes because of the interaction between amphiphiles and enhance the interfacial and micellar properties.[27] In this study, the use of **8** in mixed micelle solutions with the conventional anionic surfactant SDS as well as the cationic surfactant CTAB has been investigated. The CMC values of the different binary combinations of SDS/CTAB and **8** are presented in Table 5.

The CMC values of the binary mixtures were lower compared to the CMC of the pure SDS or CTAB solution, suggesting that micellar formation is more favored in the mixed micellar system. This is mainly due to the electronic charge screening of the anionic head group of SDS and cationic moiety of CTAB by the nonionic molecules of **8**, causing less repulsion between the molecules.

The ideal CMC of the SDS/CTAB–**8** binary mixture can be predicted by the Clint equation[28] (Equation 3):

$$\frac{1}{\text{cmc}^*} = \frac{\alpha_8}{\text{cmc}_8} + \frac{(1-\alpha_8)}{\text{cmc}_{\text{SDS/CTAB}}} \quad (3)$$

where α_8 is the mole fraction of the **8** in the mixture, cmc_8 and $\text{cmc}_{\text{SDS/CTAB}}$ correspond to the critical micelle concentrations of pure components **8** and SDS or CTAB, respectively, and cmc* is the value under ideal mixing.

TABLE 4 Critical micelle concentration and aggregation number of N-acyl tyrosine surfactants

Compound	Chain Length: Double Bonds	CMC Value (μM)	Aggregation Number (*N*ss)
2	10:0	203	6
3	12:0	117	13
4	14:0	25	17
5	16:0	18	18
6	18:0	10	22
7	18:1	22	12
8	12:0	50	20

Abbreviation: CMC, critical micelle concentration.

TABLE 5 CMC of SDS/CTAB–8 mixed system

Mole Fraction				
Surfactant 8	SDS	CMC (μM)	CTAB	CMC (μM)
0	1	8300	1	917
0.2	0.8	462	0.8	148
0.4	0.6	246	0.6	77
0.6	0.4	113	0.4	39
0.8	0.2	95	0.2	19
1	0	50	0	50

Abbreviations: CMC, critical micelle concentration; CTAB, cetyl trimethyl ammonium bromide; SDS, sodium dodecyl sulfate.

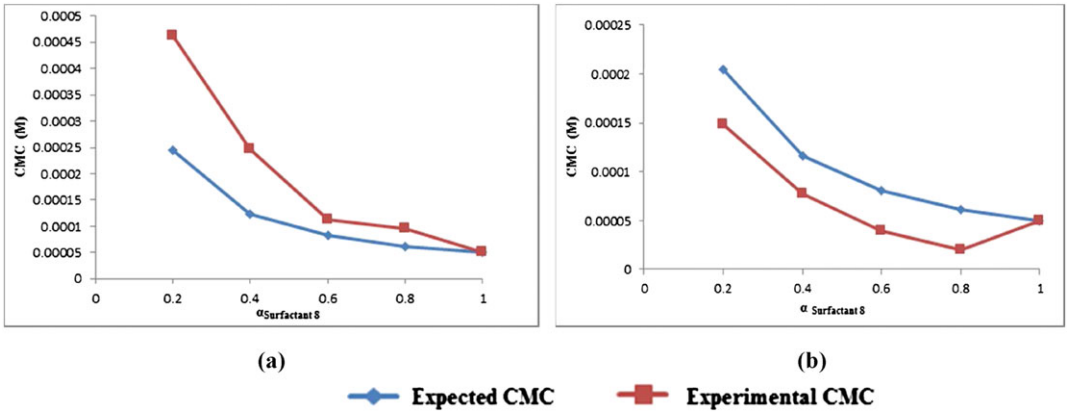

FIGURE 7 Variation of CMC with mole fraction of surfactant **8** in (A) SDS and (B) CTAB mixed systems. CMC indicates critical micelle concentration; CTAB, cetyl trimethyl ammonium bromide; SDS, sodium dodecyl sulfate

The micellar molar fraction of **8** in the ideal state $\chi_8^{id}$was evaluated according to Equation 4, assuming binary ideal mixture.

$$\chi_8^{id} = \frac{\alpha_8 cmc_{SDS/CTAB}}{\alpha_8 \mathrm{cmc}_{\mathrm{SDS/CTAB}} + (1-\alpha_8)\mathrm{cmc}_8}. \quad (4)$$

The experimental value and theoretical value predicted by the Clint equation for the CMC of each of the surfactant binary mixtures are shown in Figure 7.

The experimental CMC values of **8** in a mixture of SDS and CTAB showed a slight deviation from the values predicted by the Clint model as can be seen from Figure 6, suggesting nonideal behavior in the mixed micellar system. The CMC values obtained for the SDS-**8** binary system were slightly higher than those predicted by the Clint model that suggested antagonistic behavior in the binary system. However, in the case of CTAB-surfactant binary mixture, the experimental CMC was lower than those predicted by the Clint model suggesting synergism in the mixed micelle formation.

The extent of nonideality of surfactant interactions is usually evaluated using the regular solution theory that includes an interaction parameter, β_{12}, to characterize the interactions between the 2 components within the mixed micelles. This parameter is related to the activity coefficients, f, of the surfactants within the micelle, according to

$$f_1 = \exp\beta_{12}(1-\chi 8)^2, \quad (5)$$

$$f_2 = \exp\beta_{12}\chi 8, \quad (6)$$

where χ_8, the molar fraction of **8** in the mixed micelle, can be obtained by solving the following equation iteratively:

$$\frac{\chi_8^2 \ln(\alpha_8 \mathrm{cmc}/\chi_8 \mathrm{cmc}_8)}{(1-\chi_8)^2 \ln[(1-\alpha_8)\mathrm{cmc}/(1-\chi_8)\mathrm{cmc}_{\mathrm{SDS}}} = 1. \quad (7)$$

The interaction parameter β_{12} can then be evaluated from

$$\beta_{12} = \frac{\ln(\alpha_8 \mathrm{cmc}/\chi_8 \mathrm{cmc}_8)}{(1-\chi_8)^2}. \quad (8)$$

From the equation, it is possible to obtain the molar fraction of **8** in the mixed micelle, χ_8 as a function of the surfactant molar fraction in bulk.

The amount of surfactant **8** in the mixed micelle is superior to the value predicted for ideal mixing (Equation 3), suggesting that the surfactant **8** becomes more prominent in the mixed micelle become richer with than with CTAB or SDS.

A negative β_{12} value accounts for synergism while a positive value indicates antagonism behavior for the mixed micelle formation.[29] In the SDS-**8** system, positive β_{12} values (0.57 to 8.85) were obtained from the different mole ratios studied that indicates the antagonistic behavior within the mixed micelle. However, for CTAB-**8** system, negative β_{12} values (−3.30 to −15.33) were obtained that confirms synergistic effect within the binary system.

3.3 | Krafft temperature

The micelle forming ability of surfactants is responsible for their surface active and detergent properties, rendering them useful in many applications. However, surfactants exhibit their micellar properties only above a certain temperature called the Krafft temperature (T_K), which is defined as the minimum temperature above which the surfactants are able to form micelles in aqueous solution.[30] Therefore, it is essential to lower the T_K of surfactants inferior to room temperature to be able to render them practical for pharmaceutical and industrial use.[31] In this study, the T_K of the synergistic CTAB-**8** mixtures with varying mole fractions of **8** was studied. The T_K of the mixtures was taken by the abrupt change in conductivity versus temperature plot (Figure 8).

In pure water, the T_K value obtained for CTAB was found to be 22°C that is comparable to that reported in previous report.[31] The T_K of pure surfactant **8** could not be obtained since it is uncharged and therefore it does not have a conductivity value. Usually, addition of electrolytes or surfactants that lower the CMCs of surfactants tends to increase their T_K rendering them impractical for many applications.[32] However, in this study, addition of surfactant **8** lowered the T_K of CTAB. Increase in mole fraction of surfactant **8** from

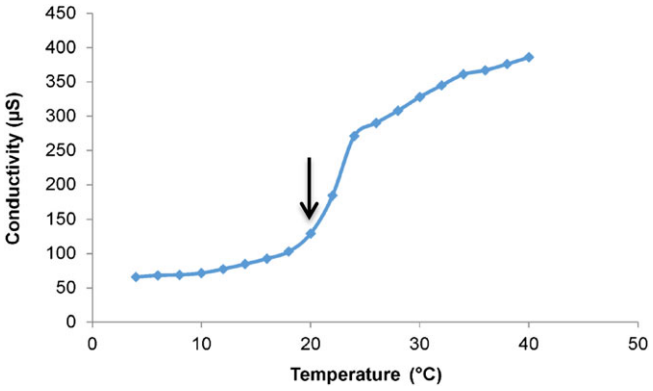

FIGURE 8 Krafft temperature of cetyl trimethyl ammonium bromide–**8** system with $\alpha_{\mathbf{8}} = 0.2$. The arrow indicates the Krafft temperature

$\alpha_{\mathbf{8}} = 0$ to $\alpha_{\mathbf{8}} = 0.8$ gradually decreased the T_K from 22°C to 12°C (Figure 9) that might be due to the increase in synergism in the mixed micelle that facilitates micelle formation at a lower temperature.

3.4 | Antibacterial activity

The antibacterial activity of the N-acyl surfactants was determined, and the MICs are given in Table 6.

Overall, the N-acyl surfactants displayed moderate to good antibacterial activity. Among the straight chain surfactants tested, the C_{12} derivative (**3**) displayed the best activity among the series. The mechanism of activity is suggested to be associated with their intercalation into target cell membrane that causes disturbance in some membrane processes leading to cell death.

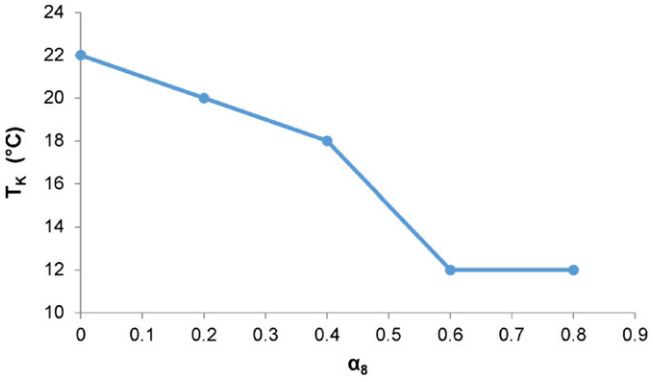

FIGURE 9 Effect of surfactant **8** on T_K of cetyl trimethyl ammonium bromide–**8** mixture

Presence of a *cis* double bond in **7** enhanced the antibacterial activity over **6**, which is the saturated analogue of **7** with the same number of carbon atom (C_{18}). The enhanced antibacterial activity of compound **7** can be attributed to its better solubility compared to the saturated stearoyl analogue and is more likely to possess the right lipophilic/hydrophilic balance that allows the molecule to disrupt the cell membrane of the microorganism as suggested by Birnie et al.[33]

The Gemini surfactant **8** that consists of 2 alkyl chains with 12 carbon atoms displayed enhanced antibacterial activity because of an increase in the hydrophobic interaction between the surfactant molecule and the bacterial membrane. The surfactant **8** showed the best activity towards *B cereus* among the gram-positive bacteria tested while *K pneumonia* was the most susceptible among the gram-negative strains.

Subsequently, the antibacterial activity of the binary mixture of **8**, with conventional anionic and cationic surfactants SDS and CTAB, respectively, was evaluated against *B cereus* and *K pneumonia*. The results are shown in Table 7.

Overall, the CTAB-**8** binary mixture showed better antibacterial activity compared to that of the SDS-**8** mixture. Sodium dodecyl sulfate and **8** exhibited comparable antimicrobial properties against the bacteria tested. It was found that for the SDS-**8** binary mixture, an increase in mole fraction of **8** from 0 to 0.2 increases the antibacterial activity and further increase in $\alpha_{\mathbf{8}}$ causes a decrease in the antibacterial activity. In the case of CTAB-**8** binary mixture, an increase in the mole fraction of **8** increases the antibacterial activity up to $\alpha_{\mathbf{8}} = 0.6$ and then decreases with further increase in mole fraction of **8**.

To be able to evaluate the activity of combinations of agents, fractional inhibitory concentration (FIC) indices were calculated using the following formula:

$$FIC = (MIC_{\mathbf{8}}^{*}/MIC_{\mathbf{8}} \text{ alone}) + (MIC_{SDS \text{ or } CTAB}^{*} \text{ in combination}/MIC_{SDS \text{ or } CTAB}),$$

where $MIC_{\mathbf{8}}^{*}$ and $MIC_{SDS \text{ or } CTAB}^{*}$ are the MICs of **8** and SDS/CTAB in combination, respectively; $MIC_{\mathbf{8}}$ and $MIC_{SDS \text{ or } CTAB}$ are the MICs of **8** and SDS/CTAB, respectively.

TABLE 6 Minimum inhibitory concentration of the N-acyl Tyrosine surfactants

		MIC (mM)							
Microorganisms		**2**	**3**	**4**	**5**	**6**	**7**	**8**	**CTAB**
Gram positive	*S aureus*	6.25	1.56	12.5	12.5	12.5	1.17	0.78	13.39
	S epidermidis	6.25	0.78	9.38	12.5	12.5	1.56	0.78	3.35
	B cereus	12.5	1.56	3.13	12.5	12.5	3.13	0.15	3.35
Gram negative	*K pneumoniae*	6.25	6.25	6.25	6.25	6.25	1.56	3.13	53.5
	P aeruginosa	6.25	6.25	9.38	9.38	12.5	3.13	6.25	62.5
	S typhimurium	9.38	6.25	12.5	12.5	9.38	3.13	6.25	53.5

Abbreviation: CTAB, cetyl trimethyl ammonium bromide; MIC, minimum inhibitory concentration.

TABLE 7 Antibacterial activity of surfactant **8** in SDS and CTAB mixtures

		MIC (mM)					
	Mole Fraction Surfactant 8	**0**	**0.2**	**0.4**	**0.6**	**0.8**	**1**
B cereus	SDS	0.195	0.097	0.293	0.390	0.390	0.15
	CTAB	0.003	0.003	0.002	0.0015	0.0183	0.15
K pneumoniae	SDS	1.56	0.39	0.59	0.78	3.12	3.13
	CTAB	0.037	0.048	0.073	0.39	3.12	3.12

Abbreviations: CTAB, cetyl trimethyl ammonium bromide; MIC, minimum inhibitory concentration; SDS, sodium dodecyl sulfate.

The interpretation made was as follows: for synergy FIC $\leq$ 0.5; partial synergy FIC > 0.5 but <1; and additive FIC = 1.0 and antagonistic when values were >1.0.[34,35] The classification of surfactant **8** in the different surfactant mixtures is shown in Table 8.

From the FIC values with respect to *B cereus*, it was found that in the SDS mixture, **8** has an additive effect at mole fraction 0.2 and displayed antagonistic effect with further increase in mole fraction. The CTAB-**8** mixtures showed additive behavior at mole fraction $\alpha_{\mathbf{8}} = 0.2$, displaying partial synergism to synergistic behavior with increasing mole fraction of 8 up to 0.6. However, further increase in $\alpha_{\mathbf{8}}$ resulted in antagonistic behavior. In the case of *K pneumonia*, the SDS mixture showed synergism to partial synergism at mole fraction $\alpha_{\mathbf{8}} = 0.2$ to 0.6 and showed antagonism at mole fraction $\alpha_{\mathbf{8}} = 0.8$. The CTAB mixtures showed antagonistic effect against *K pneumonia*.

3.5 | Foaming ability

Foaming is a special feature of surfactants that makes them useful in different applications, such as household detergents and cosmetics. The N-acyl tyrosine surfactants were found to possess promising antibacterial activity as single or mixed systems. In view of investigating their potential use in detergent formulations, their foamability was investigated. In general, the N-acyl tyrosine surfactants were found to have very poor foaming ability.

Addition of SDS or CTAB to an aqueous solution of **8** was found to enhance the foaming ability of the solution (Figure 10). Surfactant **8**-CTAB mixtures showed better foaming ability compared to surfactant **8**-SDS mixtures. This may be due to the synergistic behavior of the surfactant **8**-CTAB mixed system, which enhances the foaming ability of the mixture compared to surfactant **8**-SDS mixture that displays antagonistic behavior. Hence, it may be assumed that in this case, synergism plays an important role in the foaming ability of the mixed surfactant systems.

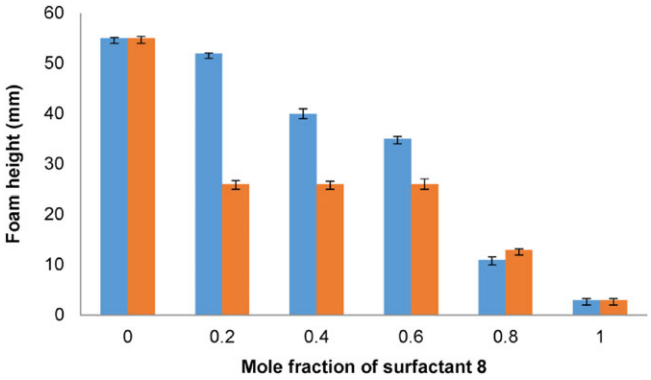

FIGURE 10 Foaming ability of surfactant **8** in CTAB and SDS mixtures. CTAB indicates cetyl trimethyl ammonium bromide; SDS, sodium dodecyl sulfate

3.6 | Hemolytic activity and ocular irritation

The red blood cell assay is a renowned method used for the estimation of potential irritation of surfactants and detergents. This method has been known to provide reliable results on the in vitro effects of test substances without involving the use of animal testings. The red blood cell assay is based on the degree of hemolysis and cell protein denaturation caused by the surfactants and the ratio of both parameters.[36]

The binary mixture of the surfactant **8**, with conventional anionic and cationic surfactants SDS and CTAB, respectively, was found to possess interesting physicochemical and antibacterial activities. To be able to evaluate the

TABLE 8 FIC indices

Mole Fraction of 8	FIC (*B cereus*) in Combination with CTAB	Inference	FIC (*K pneumoniae*) in Combination with CTAB	Inference	FIC (*B cereus*) in Combination with SDS	Inference	FIC (*K pneumoniae*) in Combination with SDS	Inference
0.2	1.00	Additive	1.31	Antagonistic	1.1	Additive	0.37	Synergistic
0.4	0.68	Partial synergy	1.99	Antagonistic	3.5	Antagonistic	0.57	Partial synergy
0.6	0.50	Synergistic	10.7	Antagonistic	4.6	Antagonistic	0.75	Partial synergy
0.8	6.20	Antagonistic	85.5	Antagonistic	4.6	Antagonistic	2.00	Antagonistic

Abbreviation: CTAB, cetyl trimethyl ammonium bromide; FIC, fractional inhibitory concentration; SDS, sodium dodecyl sulfate.

TABLE 9 Hemolytic activity and in vitro classification of compound **8** in SDS and CTAB surfactant mixtures

$\alpha_{\text{compound 8}}$	HC_{50} in CTAB (μg mL^{-1})	DI %	*L/D* Ratio	In Vitro Classification	HC_{50} in SDS (μg mL^{-1})	DI %	*L/D* Ratio	In Vitro Classification
0	1.82	22	0.08	Irritant	43.6	100	0.4	Irritant
0.2	191	95	2	Moderate irritant	203	16.5	12.3	Weak irritant
0.4	300	71.7	4	Moderate irritant	347	70.2	4.94	Moderate irritant
0.6	233	25	9.32	Moderate irritant	350	23.3	15.0	Weak irritant
0.8	215	68	3.16	Moderate irritant	356	65.0	5.47	Moderate irritant
1	159.3	62	2.57	Moderate irritant	159.3	62	2.57	Moderate irritant

Abbreviation: CTAB, cetyl trimethyl ammonium bromide; SDS, sodium dodecyl sulfate.

potential safety of these mixed surfactant combinations as detergent formulations, their hemolytic activity and denaturation ability were evaluated on human red blood cells. The HC_{50}, denaturation index, and the in vitro classification of the different mixed micelle combinations are shown in Table 9.

Pure CTAB and pure SDS are irritants and addition of **8** causes a decrease in the irritancy of the mixed surfactant systems. The CTAB-**8** mixture showed moderate irritancy while the SDS-**8** mixture displayed moderate to weak irritancy. In both CTAB and SDS mixtures, the mixed system consisting of $\alpha_{\mathbf{8}} = 0.6$ displayed the lowest irritation index among all the surfactant mixtures studied.

4 | CONCLUSION

N-acyl surfactants with varying chain length were successfully synthesized in good yields. Increasing the chain length of the hydrophobic portion of the surfactants favors micellar formation while the presence of an unsaturated system was found to decrease the ease of micellization. The N-acyl tyrosine surfactants showed moderate to good antibacterial activity that was affected by both chain length and level of unsaturation of the hydrophobic tail. Among the single chain N-acyl surfactants, the C_{12} derivative (surfactant **3**) displayed the highest antibacterial activity. The presence of double bond in the oleoyl derivative enhanced the antibacterial activity over its saturated analogue. The Gemini surfactant **8** displayed the highest activity among all the compound tested. The study of binary mixtures of compound **8** with conventional surfactants shows that surfactant **8** displayed antagonistic behavior in SDS and synergistic behavior in CTAB mixed micellar systems. The synergistic CTAB-**8** mixtures displayed better antibacterial activity and foaming properties than the SDS-**8** mixtures. The CTAB-**8** mixture with $\alpha_{\mathbf{8}} = 0.4$ to 0.6 showed the highest antibacterial activity and lowest ocular irritation index that makes it a good candidate in its use as detergents and antiseptic.

ACKNOWLEDGEMENTS

One of the authors is thankful to Tertiary Education Commission of Mauritius for the grant of Scholarship.

REFERENCES

[1] I. A. Nnanna, J. Xia, *Protein Based Surfactants: Synthesis, Physicochemical Properties and Applications, Surfactant Science Series, 101*, Marcel Dekker, New York, USA **1998**.

[2] N. Chandra, V. K. Tyagi, *J. Dispersion Sci. Technol.* **2013**, *34*, 800.

[3] M. R. Infante, L. Perez, A. Pinazo, P. Clapes, M. C. Moran, M. Angelet, M. T. Garcia, M. P. Vinardell, *C. R. Chim.* **2004**, *7*, 583.

[4] R. Bordes, K. Holmberg, *Adv. Colloid Interface Sci.* **2015**, *222*, 79.

[5] G. Ray, S. Ghosh, S. Moulik, *J. Surfactants Deterg.* **2009**, *12*, 131.

[6] W. Qiao, Y. Qiao, *J. Surfactants Deterg.* **2013**, *16*, 821.

[7] A. Ohta, K. Toda, Y. Morimoto, T. Asakawa, S. Miyagishi, *Colloids Surf., A* **2008**, *317*, 316.

[8] A. Laschewski, *Tenside Surfact Det* **2003**, *40*, 246.

[9] J. Xia, Y. Xia, I. A. Nnanna, *J Agri Food Chem.* **1995**, *43*, 867.

[10] A. Nagao, M. Kito, *J. Am. Oil Chem. Soc.* **1989**, *66*, 710.

[11] M. Sreenu, R. R. Nayak, R. B. N. Prasad, *Colloids Surf., A* **2014**, *449*, 74.

[12] D. R. Perinelli, L. Casettari, M. Cespi, F. Fini, D. K. W. Man, G. Giorgioni, S. Canala, J. K. W. Lam, G. Bonacucina, G. F. Palmieri, *Colloids Surf., A* **2016**, *492*, 38.

[13] A. Ohta, R. Daner, K. Nagayama, T. Mita, T. Asagawa, S. Miyagishi, *Langmuir* **2006**, *22*, 8472.

[14] A. Ohta, K. Tani-I, A. Hoshiba, T. Asagawa, S. Miyagishi, *Chem. Lett.* **2005**, *34*, 560.

[15] N. Joondan, S. Jhaumeer-Laulloo, P. Caumul, *Microbiol. Res.* **2014**, *169*, 675.

[16] Bruker. *APEX2, SAINT and SADABS*. Bruker AXS Inc., Madison, Wisconsin, USA, **2012**.

[17] G. M. Sheldrick, *Acta Cryst.* **2015**, *C71*, 3.

[18] L. J. Farrugia, *J. Appl. Crystallogr.* **2012**, *45*, 849.

[19] M. E. Fait, G. L. Garrote, P. Clapes, S. Tanco, J. Lorenzo, S. R. Morcelle, *Amino Acids* **2015**, *47*, 1465.

[20] R. Bordes, J. Tropsch, K. Holmberg, *J Colloid and Interface Science.* **2009**, *338*, 529.

[21] M. P. Akerman, V. A. Chiazzari, *J. Mol. Struct.* **2014**, *1058*, 22.

[22] C. Pineiro, M. Novo, W. Al-Soufi, *Adv Colloid Int Sci.* **2015**, *215*, 1.

[23] B. M. Folmer, K. Holmberg, E. Gottberg Klingskog, K. Bergstrom, *J Surfact Deterg.* **2001**, *4*, 175.

[24] K. Holmberg, *Novel Surfactants: Preparation, Application and Biodegradability, in Surfactant Science Series*, 2nd ed., Marcel Dekker, New York, USA **2004**.

[25] P. M. Holland, D. N. Rubingh, *ACS Symp. Ser.* **1992**, *501*, 2.

[26] C. P. Ong, C. L. Ng, H. K. Lee, S. F. Y. Li, *Electrophoresis* **1994**, *15*, 1273.

[27] L. G. Chen, H. Bermudez, *Langmuir* **2013**, *29*, 2805.

[28] J. H. Clint, *Surfactant Aggregation*, Chapman and Hall, New York **1992**.

[29] C. M. C. Faustino, A. R. T. Calado, L. Garcia-Rio, *J. Colloid Interface Sci.* **2011**, *329*, 493.

[30] Z. Chu, Y. Feng, *Langmuir* **2012**, *28*, 1175.

[31] J. C. Roy, M. N. Islam, G. Aktaruzzaman, *J Surfact Deterg* **2013**, *17*, 231.

[32] T. W. Davey, W. A. Ducker, A. R. Hayman, J. Simpon, *Langmuir* **1998**, *14*, 3210.

[33] C. R. Birnie, D. Malamud, R. L. Schnaare, *Antimicrob. Agents Chemother.* **2000**, *44*, 2514.

[34] K. E. Sook, S. I. Jeong, J. H. Kim, C. Park, S. M. Kim, J. L. Kim, K. M. Lee, S. H. Lee, H. So, R. Park, *J. Microbiol. Biotechnol.* **2009**, *19*, 1576.

[35] K. A. Kumar, K. Mazumdar, N. K. Dutta, P. Karak, S. G. Datidar, R. Ray, *Biol. Pharm. Bull.* **2004**, *27*, 1116.

[36] W. J. W. Pape, U. Hopper, *Drug Res.* **1990**, *4*, 498.

SUPPORTING INFORMATION

Additional Supporting Information may be found online in the supporting information tab for this article.

How to cite this article: Joondan N, Jhaumeer-Laulloo S, Caumul P, and Akerman M. Synthesis, physicochemical, and biological activities of novel N-acyl tyrosine monomeric and Gemini surfactants in single and SDS/CTAB–mixed micellar system. *J Phys Org Chem*. 2016. doi: 10.1002/poc.3675